RESEARCH ARTICLE

A human coronavirus evolves antigenically to escape antibody immunity

Rachel T. Eguia[1], Katharine H. D. Crawford[1,2,3], Terry Stevens-Ayers[4],
Laurel Kelnhofer-Millevolte[3], Alexander L. Greninger[4,5], Janet A. Englund[6,7], Michael
J. Boeckh[4], Jesse D. Bloom[1,2,8]*

1 Basic Sciences and Computational Biology, Fred Hutchinson Cancer Research Center, Seattle,
Washington, United States of America, 2 Department of Genome Sciences, University of Washington,
Seattle, Washington, United States of America, 3 Medical Scientist Training Program, University of
Washington, Seattle, Washington, United States of America, 4 Vaccine and Infectious Diseases Division,
Fred Hutchinson Cancer Research Center, Seattle, Washington, United States of America, 5 Department of
Laboratory Medicine and Pathology, University of Washington, Seattle, Washington, United States of
America, 6 Seattle Children's Research Institute, Seattle, Washington, United States of America,
7 Department of Pediatrics, University of Washington, Seattle, Washington, United States of America,
8 Howard Hughes Medical Institute, Seattle, Washington, United States of America

* jbloom@fredhutch.org

Abstract

There is intense interest in antibody immunity to coronaviruses. However, it is unknown if
coronaviruses evolve to escape such immunity, and if so, how rapidly. Here we address this
question by characterizing the historical evolution of human coronavirus 229E. We identify
human sera from the 1980s and 1990s that have neutralizing titers against contemporane-
ous 229E that are comparable to the anti-SARS-CoV-2 titers induced by SARS-CoV-2 infec-
tion or vaccination. We test these sera against 229E strains isolated after sera collection,
and find that neutralizing titers are lower against these "future" viruses. In some cases, sera
that neutralize contemporaneous 229E viral strains with titers >1:100 do not detectably neu-
tralize strains isolated 8–17 years later. The decreased neutralization of "future" viruses is
due to antigenic evolution of the viral spike, especially in the receptor-binding domain. If
these results extrapolate to other coronaviruses, then it may be advisable to periodically
update SARS-CoV-2 vaccines.

Author summary

Hopes for controlling SARS-CoV-2 rely on vaccination or infection to confer immunity
that protects against subsequent infection. However, the "common-cold" seasonal corona-
viruses re-infect people every few years. It has been unclear if these re-infections occur
because immunity wanes rapidly, or because the virus evolves to escape immunity elicited
by prior infection. Here we investigate the second hypothesis in the context of the com-
mon-cold coronavirus 229E. We test how well antibodies in old human sera neutralize
both contemporaneous old 229E viruses, and more recent viruses that evolved after the
sera was collected. We find that as 229E evolves, its spike protein accumulates mutations
that escape neutralization by older human sera. The rate at which viral evolution degrades

immunity varies among individuals, but in some cases less than a decade of evolution is sufficient to completely eliminate neutralization by human sera that is potent against contemporaneous viruses. Many of the viral mutations occur in the same regions of the spike (the RBD and NTD) that are changing in emerging variants of SARS-CoV-2. Therefore, our results suggest that coronavirus vaccines may need to be periodically updated to keep pace with viral evolution.

Introduction

The SARS-CoV-2 pandemic has caused an urgent need to determine how well antibody immunity protects against SARS-CoV-2 infection. The evidence so far is promising. Neutralizing and anti-spike antibodies elicited by natural infection correlate with reduced SARS-CoV-2 infection of humans [1,2], and vaccines that elicit such antibodies protect humans with high efficacy [3]. These findings in humans are corroborated by a multitude of animal studies showing that neutralizing antibodies to the SARS-CoV-2 spike protect against infection and disease [4–7].

However, humans are repeatedly re-infected with the "common-cold" coronaviruses 229E, OC43, HKU1, and NL63 [8–10]. For instance, serological studies suggest that the typical person is infected with 229E every 2–3 years [8,10], although a lower infection rate and no 229E re-infections were reported in a 4-year study that identified infections by the criteria of a positive PCR test in the context of respiratory illness [11]. In any case, the fact that common-cold coronavirus re-infections occur at some appreciable rate has led to concerns that coronavirus immunity is not "durable." These concerns initially focused on the possibility that the immune response itself is not durable [12]. This possibility now seems less likely, as SARS-CoV-2 infection induces neutralizing antibodies and memory B cells with dynamics similar to other respiratory viruses [13–16].

But there is another mechanism by which viruses can re-infect even in the face of long-lived and effective antibodies: antigenic evolution. For example, infection with influenza virus elicits antibodies that generally protect humans against that same viral strain for at least several decades [17,18]. Unfortunately, influenza virus undergoes rapid antigenic evolution to escape these antibodies [19], meaning that although immunity to the original viral strain lasts for decades, humans are susceptible to infection by its descendants within about 5 years [17,20]. This continual antigenic evolution is the reason that the influenza vaccine is periodically updated.

Strangely, the possibility of antigenic evolution by coronaviruses has received only modest attention, perhaps because coronaviruses have lower mutation rates than other RNA viruses [21,22]. However, mutation rate is just one factor that shapes antigenic evolution; influenza and measles virus both have high mutation rates, but only the former undergoes rapid antigenic evolution. Furthermore, the assumption of minimal coronavirus antigenic evolution is not supported by the limited evidence to date. In the 1980s, human-challenge studies found that individuals infected with one strain of 229E were resistant to re-infection with that same strain, but partially susceptible to a different strain [23]. Additional experimental studies suggest that sera or antibodies can differentially recognize spike proteins from different 229E strains [24,25]. From a computational perspective, several studies have reported that the spikes of 229E and OC43 evolve under positive selection [26–28], which is often a signature of antigenic evolution.

Here we experimentally assess whether coronavirus 229E escapes neutralization by human polyclonal sera by reconstructing the virus's evolution over the last several decades. We show

that historical sera that potently neutralize virions pseudotyped with contemporaneous 229E spikes often have little or no activity against spikes from 229E strains isolated 8–17 years later. Conversely, modern sera from adults generally neutralize spikes from a wide span of historical viruses, whereas modern sera from children best neutralize spikes from recent viruses that circulated during the children's lifetimes. These patterns are explained by antigenic evolution of the spike, especially within the receptor-binding domain. If SARS-CoV-2 undergoes similarly rapid antigenic evolution, then it may be advisable to periodically update vaccines to keep pace with viral evolution.

Results

Phylogenetic analysis of 229E spikes to identify historical strains for experimental study

We focused our studies on the viral spike protein because it is the main target of neutralizing antibodies [29], and because anti-spike antibodies are the immune parameter best established to associate with protection against coronavirus infection in humans [1–3,30,31].

Because SARS-CoV-2 has circulated in humans for just over a year, we needed to choose another coronavirus with a more extensive evolutionary history. Of the four human-endemic common-cold coronaviruses, the two alphacoronaviruses 229E and NL63 are similar to SARS-CoV-2 in binding a protein receptor via the spike's receptor-binding domain (RBD, also known as S1-B) [6,32,33]. In contrast, the two betacoronaviruses OC43 and HKU1 bind glycan receptors via the spike's N-terminal domain (NTD, also known as S1-A) [34]. Antibodies that block receptor binding dominate the neutralizing activity of immunity elicited by SARS-CoV-2 infection [35–37], so we reasoned that even though SARS-CoV-2 is a betacoronavirus, its antigenic evolution is more likely to be foreshadowed by the two human alphacoronaviruses that also use their RBD to bind a protein receptor. Of these two viruses, we chose 229E since it was first identified in humans >50 years ago [38], whereas NL63 was only identified in 2003 [39].

We inferred a phylogenetic tree of 229E spikes from direct or low-passage human isolates (Fig 1A), excluding older strains passaged extensively in the lab [38]. There are several important features of the tree. First, it is clock-like, with sequence divergence proportional to virus isolation date (Figs 1A and S1). Second, the tree is "ladder-like," with short branches off a single trunk (Fig 1A). The ladder-like shape of the 229E phylogeny has been noted previously [26,27,40], and is a signature of viruses such as influenza for which immune pressure drives population turnover by selecting for antigenic variants [41–43]. Third, sequences group by date rather than country of isolation (in Fig 1A, sequences from different countries but the same year are nearby). Phylogenies that organize by date rather than geography indicate fast global transmission, another signature of human influenza virus [44,45]. Finally, although there is some intra-spike recombination, it is among closely related strains and does not affect the broader topology of the tree (S2 Fig). For our study, the key implication of the above observations is that date of virus isolation is a good proxy for evolutionary position, since 229E evolves primarily along a single trajectory through time.

For our experiments, we chose five spikes from 229E viruses spaced at roughly 8-year intervals spanning 1984 to 2016 (Fig 1A). We synthesized genes encoding all five spikes, truncating the last 19 residues of the cytoplasmic tail since this improves titers of spike-pseudotyped viruses [13,46,47]. These five spikes differ by up to 4% in amino-acid sequence over their entire lengths, but are vastly more different in their RBDs, with 17% RBD divergence between 1984 and 2016 (Fig 1B). We generated lentiviral particles pseudotyped with each spike, and found that all five supported high infectious titers in cells expressing 229E's receptor aminopeptidase
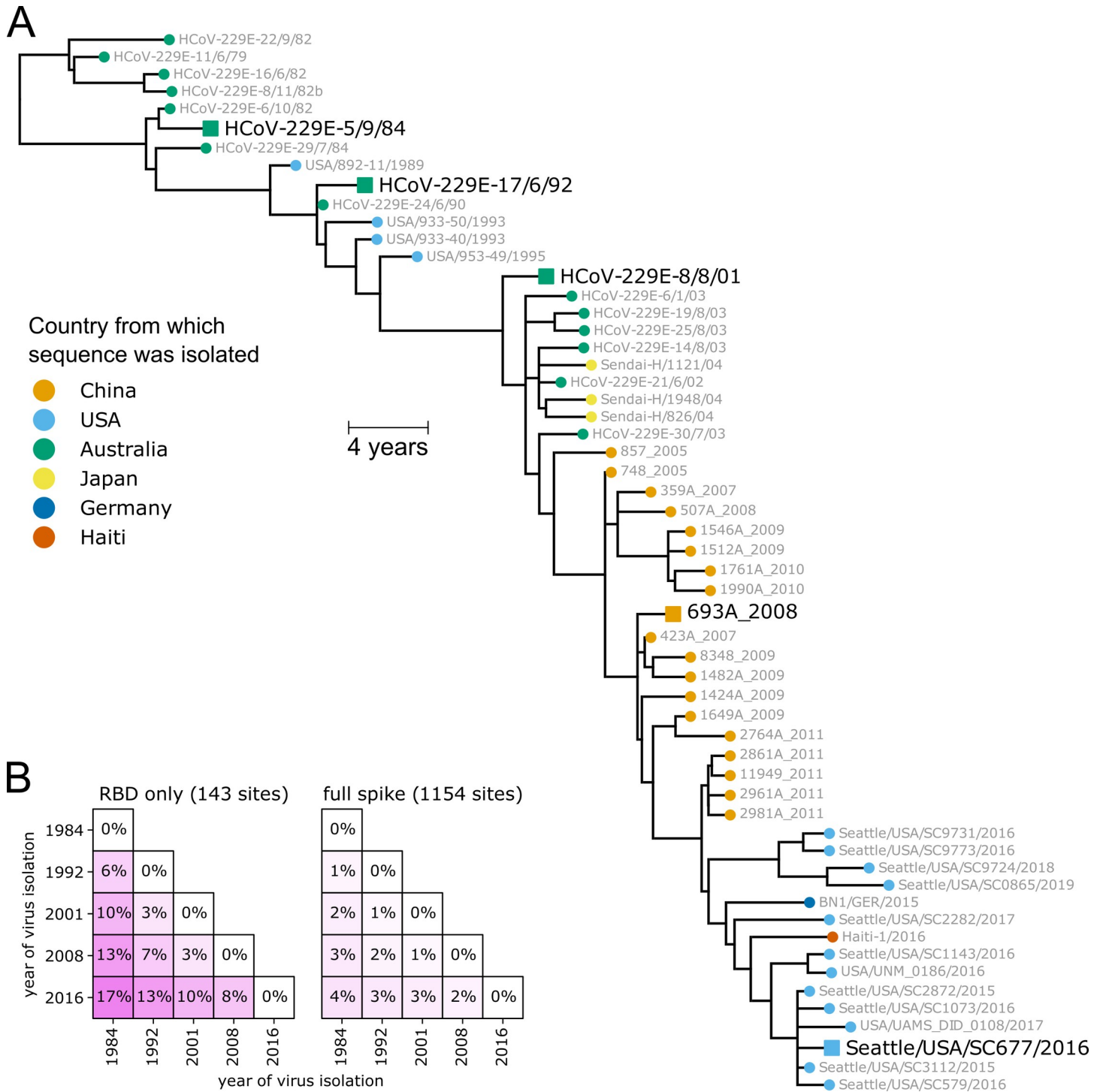
Fig 1. Spikes used in this study. (A) Phylogenetic tree of 229E spikes, with tips colored by the country from which the virus was isolated. The spikes used in the experiments are indicated with black text and square shapes. The tree is a maximum-likelihood inference with IQ-TREE [82] with a codon-substitution model and re-scaled with TreeTime [84] to position tips by to date of isolation. S1 Fig shows a tree with branch lengths proportional to divergence rather than time, and validates clock-like evolution. S2 Fig shows recombination does not substantially affect the phylogenetic placements of the spikes used in the experiments. (B) Protein sequence divergence of the spikes used in the experiments, computed over just the receptor-binding domain (RBD) or the full sequence. Divergence is the Levenshtein distance between the amino-acid sequences divided by the number of sites.

https://doi.org/10.1371/journal.ppat.1009453.g001

N [33] and the activating protease TMPRSS2 [48] (S3 Fig). Any major antigenic evolution by 229E since the 1980s should be captured by differences among these five spikes.

Neutralizing titers of historical sera drop rapidly against spikes from "future" viruses

To test if the 229E spikes had evolved to escape neutralization by human immunity, we used historical sera collected from adults between 1985 and 1990. The sera were all collected from apparently healthy individuals, and no information of recent respiratory virus infections were available (see Methods for details). Since the typical person is infected with 229E every 2–5 years [8,10,11], many of these individuals were likely infected with 1984-like viruses within a few years preceding sera collection. None of the individuals would have been infected with any of the later viruses, since those viruses did not yet exist at the time of sera collection.

Nearly all sera collected from 1985–1990 had at least some neutralizing activity against viral particles pseudotyped with the 1984 spike (25 of 27 sera had titers >1:10; S4 and S5 Figs). We focused further analysis on the roughly 30% of sera (8 of 27) that had neutralizing titers against the 1984 spike of >1:90 (S5 Fig). Our reason for focusing on these sera is that their anti-229E neutralizing titers are comparable to anti-SARS-CoV-2 sera neutralizing titers several months after recovery from COVID-19 [13,16] or receipt of the Moderna mRNA-1273 vaccine [49].

All sera that potently neutralized virions pseudotyped with the 1984 spike had reduced titers against more recent spikes (Fig 2A). In some cases, the drop in neutralization of more recent spikes was dramatic. For instance, serum collected from a 28-year old in 1990 neutralized the 1984 spike at a titer of 1:125 but did not neutralize the 1992 spike at our limit of detection of 1:10 (Fig 2A). Similarly, serum collected from a 24-year old in 1987 neutralized the 1984 spike at 1:120 but barely neutralized the 1992 spike and did not detectably neutralize spikes more recent than 1992 (Fig 2A). Only 2 of 8 sera that potently neutralized the 1984 spike detectably neutralized all subsequent spikes, and only at greatly reduced titers against the most recent spikes.

To confirm that these results reflect antigenic evolution rather than some unique neutralization susceptibility of the 1984 spike, we repeated similar experiments using sera collected from 1992–1995 and initially screening for neutralization of the 1992 spike. Again, nearly all sera (18 of 19) detectably neutralized the 1992 spike, with about a quarter (5 of 19) having titers >1:90 (S4 and S5 Figs). These potent sera also neutralized the older 1984 spike with high titers, but again generally had lower activity against spikes from viruses isolated after the sera were collected (Fig 2B). Together, the results from the two sera collection timeframes indicate that the 229E spike is evolving antigenically, such that immunity elicited by infection with prior viruses is often ineffective at neutralizing future viruses.

To quantify the rate of antigenic evolution, for all sera in Fig 2A and 2B we computed the drop in neutralization titer against spikes from one and two timepoints later relative to the contemporaneous spike. The median drop in titer was 4-fold against viruses from 8–9 years in the future, and >6-fold for viruses 16–17 years in the future (Fig 2C). However, these medians mask substantial serum-to-serum variation in neutralization of antigenically evolved future viruses. Neutralization by some sera is eroded >10-fold by just 8–9 years of viral evolution, whereas neutralization by a few sera is unaffected even by 16–17 years of evolution.

Modern sera neutralize viruses that circulated throughout an individual's lifetime

The above results show that viral antigenic evolution erodes the capacity of anti-229E immunity to neutralize the future descendants of the viruses that elicited the immunity. We next
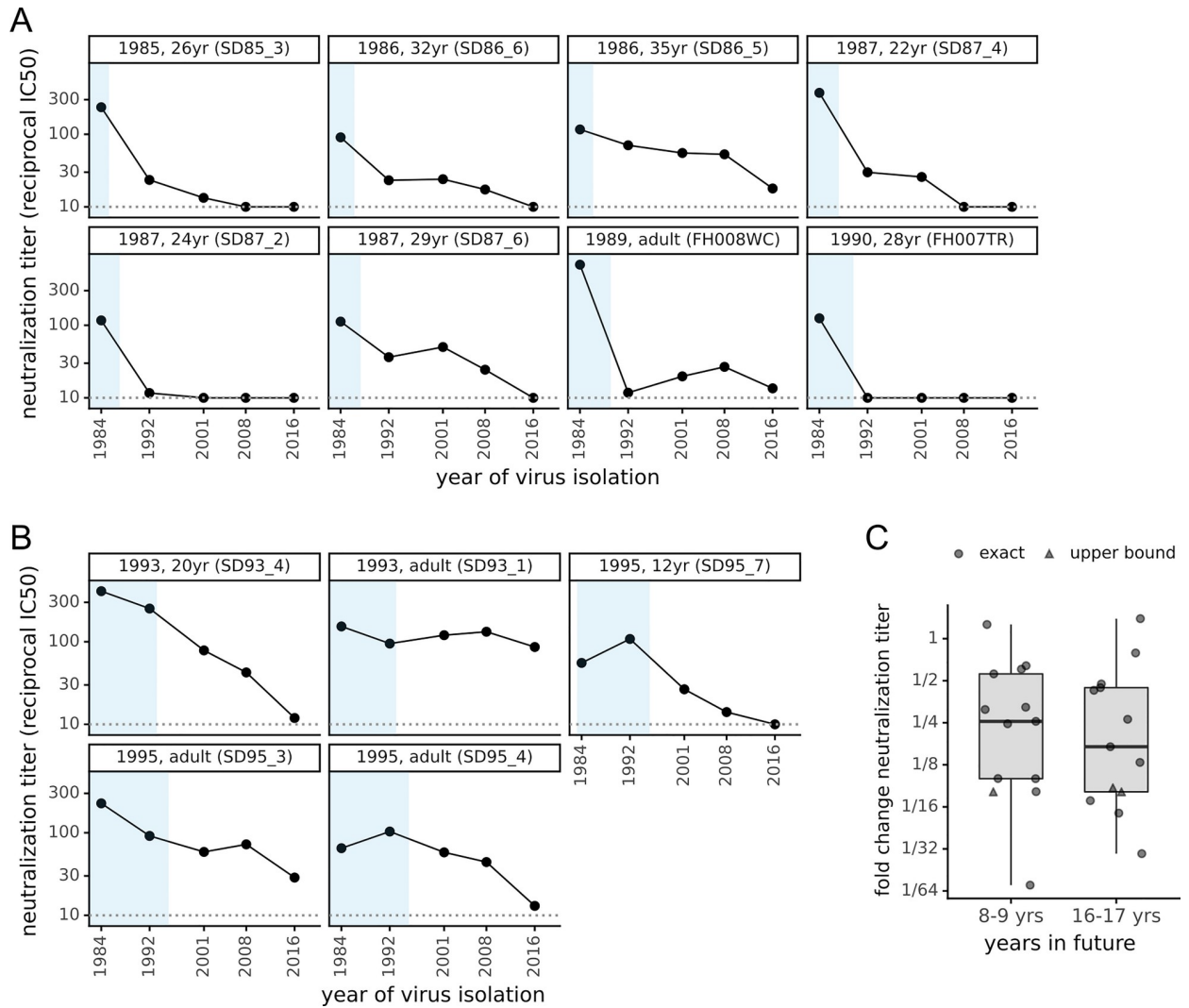
Fig 2. The neutralizing activity of human sera is lower against "future" viruses than those that elicited the immunity. (A) Sera collected between 1985 and 1990 was tested in neutralization assays against spikes from viruses isolated between 1984 and 2016. Each plot facet is a different serum, and black points show its neutralizing titer against viruses from the indicated year. Blue shading indicates the portion of plotted timeframe during which the individual could have been infected prior to serum collection. The dotted gray horizontal line indicates the limit of detection (titer of 1:10). Plot titles give the year of serum collection, the individual's age when the serum was collected, and the serum ID. (B) Plots like those in (A) but for sera collected between 1993 and 1995. (C) The fold change in neutralization titer against viruses isolated 8–9 or 16–17 years in the "future" relative to the virus isolated just before the serum was collected. Box plots show the median and interquartile range, and each point is the fold change for a single serum. For a few sera (triangles), the fold change is censored (as an upper bound) because the titer against the future virus was below the limit of detection.

addressed a related question: does serum immunity durably retain the capacity to neutralize historical 229E strains that an individual was exposed to many years ago?

To address this question, we used modern sera collected in 2020 from children and adults. The adults were alive during circulation of all five 229E spikes in our panel (i.e., they were born before 1984), but the children could only have been exposed to the more recent spikes. We screened 31 modern sera against the 2016 spike, and found that 25 of 31 detectably neutralized at a threshold of 1:10 (S4 and S5 Figs). We again focused further analysis on the more potent sera with titers >1:90 (7 of 31 sera, S5 Fig).
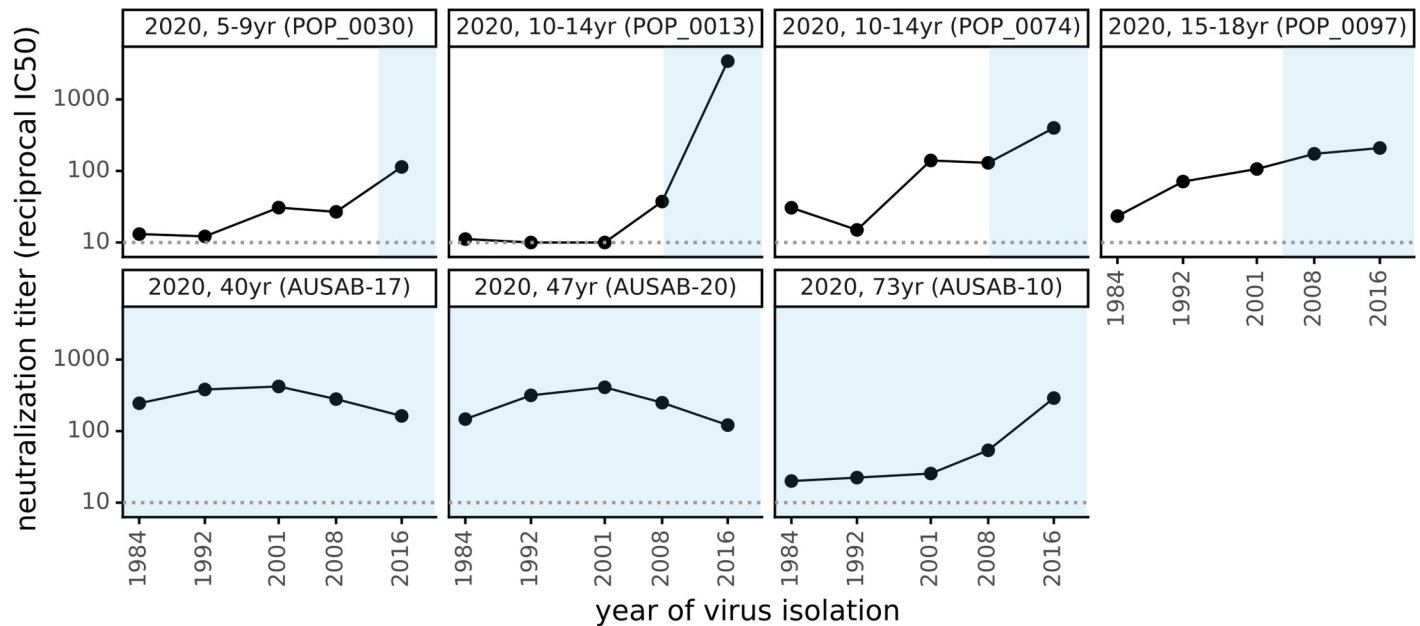
Fig 3. Neutralizing titers of sera collected in 2020 are higher against historical viruses that circulated during an individual's lifetime than viruses isolated before the individual was born. As in Fig 2A and 2B, each plot facet is a different serum with the title giving the individual's age and black points indicating the titer against spikes from viruses isolated in the indicated year. Blue shading represents the portion of the plotted timeframe during which the individual was alive: for adults this is the entire timeframe, but for children the left edge of the blue shading indicates the birth year.

Modern adult sera that potently neutralized the 2016 spike also neutralized all prior spikes dating back to 1984 (Fig 3). In contrast, the children's sera neutralized spikes from viruses that circulated during the children's lifetimes but often had reduced activity against spikes from before the children were born (Fig 3). However, neutralization by children's sera generally extends further "back in time" to viruses that preceded birth than neutralization by adult sera in Fig 2A and 2B extends "forward in time" to viruses that circulated after the sera was collected. Similar time asymmetry in antigenic evolution has been described for influenza virus [50,51]. Overall, the results in Fig 3 show that neutralizing immunity can encompass the entire spectrum of spikes an individual has been exposed to, consistent with the notion that reduced neutralization of future viruses is due to antigenic evolution rather than a lack of durability in immunity itself.

Much of the antigenic evolution is due to mutations in the spike's receptor-binding domain (RBD)

We next sought to identify the region(s) within the 229E spike where mutations drive antigenic drift. Coronavirus spikes consist of two subunits, S1 and S2, and it is well known that S2 is relatively conserved whereas S1 is more rapidly evolving [29,52]. The S1 subunit itself consists of several domains, and we were inspired by several excellent papers by Rini and colleagues to pursue the hypothesis that 229E's antigenic drift might be driven by amino-acid substitutions within the three loops in the S1 RBD that bind the cellular receptor [25,53].

We first calculated the protein sequence variability at each residue across an alignment of 229E spikes isolated between 1984 and 2019 (Fig 4A). As expected, most sequence variability was in the S1 subunit, with particularly high variability in the three receptor-binding loops within the RBD (Fig 4A). However, there was also substantial variability within some portions of the N-terminal domain (NTD) as well as other parts of the S1 subunit. The variability of each site in spike is projected onto the protein structure in Fig 4B.
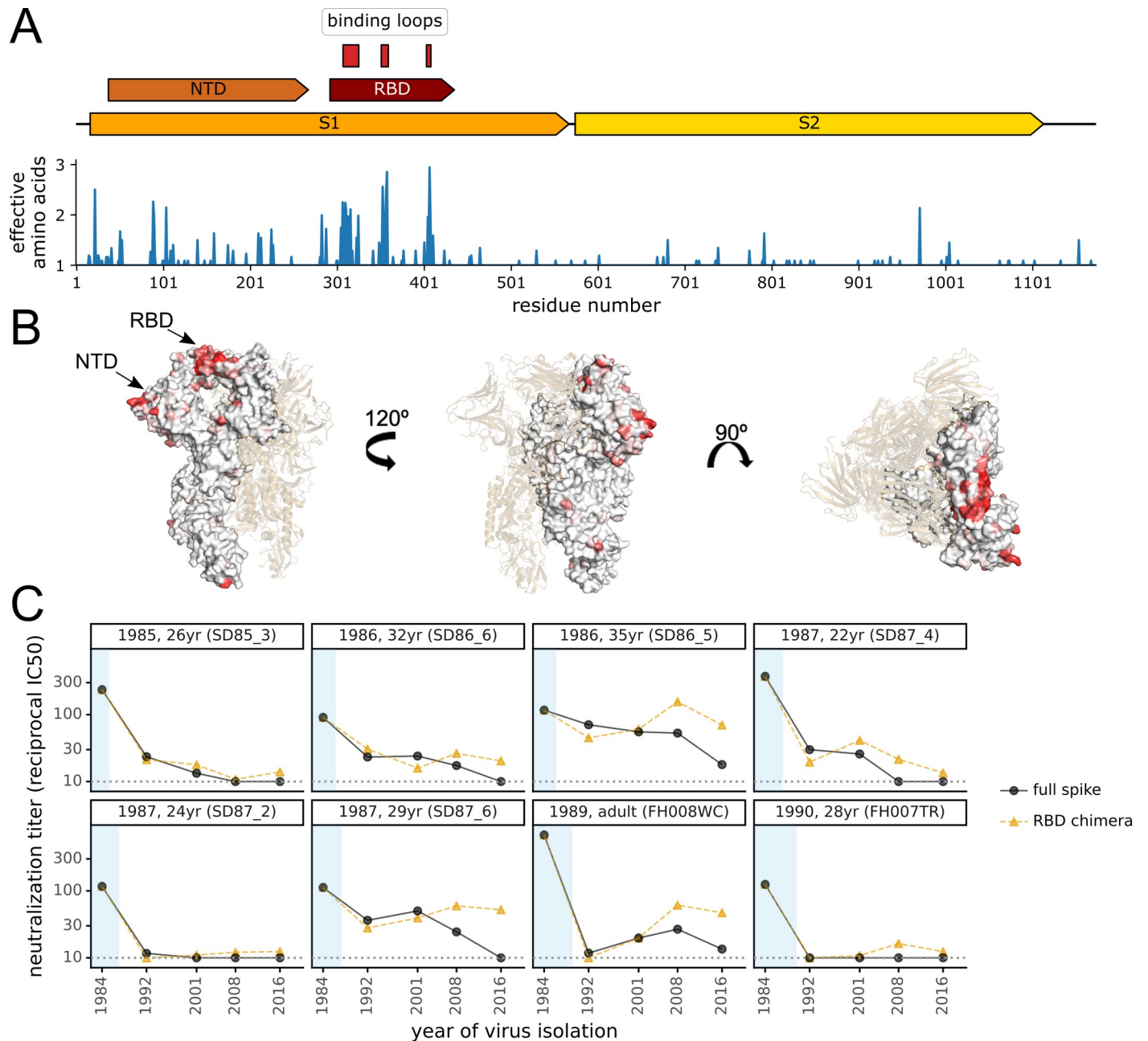
Fig 4. Antigenic evolution is primarily due to changes in the spike's receptor binding domain (RBD). (A) At top is a schematic of the 229E spike. Within the S1 subunit, the schematic indicates the N-terminal domain (NTD, also known as S1-A) and the RBD (also known as S1-B). The three loops in the RBD that bind the virus's APN receptor are indicated [53]. Below the schematic is a plot of sequence variability across the alignment of 229E spikes in Fig 1A. Variability is quantified as the effective number of amino acids at a site [86], with a value of one indicating complete conservation and larger values indicating more sequence variability. (B) Site entropy mapped on 229E spike structure (PDB 6U7H, [53]). (C) Neutralizing titers of sera collected between 1985 and 1990 against either the full spike of "future" viruses or chimeras consisting of the 1984 spike containing the RBD from "future" viruses. The plot format and the black circles (full spike) are repeated from Fig 2A with the addition of the orange triangles showing the titers against the chimeric spikes.

https://doi.org/10.1371/journal.ppat.1009453.g004

To experimentally test the extent that mutations in the RBD explained antigenic evolution, we created chimeras consisting of the 1984 spike with the RBD replaced by that of each of the four subsequent spikes. All these RBD-chimeric spikes supported efficient entry by pseudo-typed viral particles (S3 Fig). We performed neutralization assays using the chimeric spikes

against the sera from 1985–1990 that potently neutralized the 1984 spike (Fig 4C). For all sera with neutralizing activity that was rapidly eroded by antigenic evolution, the drops in titer against more recent spikes were paralleled by drops in titer against the RBD-chimeric spikes (e.g., 26 and 24-year olds in Fig 4C). However, this trend did not hold for some sera that were more resistant to antigenic evolution: for instance, serum from the 29-year old did not neutralize the 2016 spike, but neutralized the chimera with the 2016 RBD (Fig 4C). Overall, these results suggest that when the neutralizing activity of potent human sera is rapidly eroded by viral evolution this is often due to mutations within the RBD, but that antigenic evolution also occurs elsewhere in the spike. In this respect, it is worth noting that while the neutralizing activity of SARS-CoV-2 immunity elicited by infection primarily targets the RBD [36,54], mutations to the NTD also reduce neutralization by some antibodies and sera [55–62]—and some regions of the NTD undergo significant sequence evolution in 229E (Fig 4A).

Discussion

We have experimentally demonstrated that the spike of a human coronavirus evolves antigenically with sufficient speed to escape neutralization by many polyclonal human sera within one to two decades. This finding suggests that one reason that humans are repeatedly re-infected with seasonal coronaviruses may be that evolution of the viral spike erodes the immunity elicited by prior infections.

How does the rate of antigenic evolution of 229E compare to that of influenza virus? Remarkably, we could find no studies that measured how quickly influenza evolution erodes neutralization by human sera. However, numerous studies examine influenza antigenic evolution using hemagglutination-inhibition (HAI) assays with sera from ferrets infected with single viral strains [63]. The rate at which 229E escapes neutralization by human sera is several fold slower than the rate at which influenza A/H3N2 escapes HAI by ferret sera, but comparable to the rate of such escape by influenza B [19,64]. However, the sera of ferrets infected by a single influenza virus strain tend to recognize fewer viral strains than sera from humans who have been repeatedly infected with many strains [65–67]. Therefore, ferret sera HAI may overestimate how quickly influenza evolution erodes neutralization by actual human sera. For this reason, further work is needed to enable head-to-head comparisons of antigenic evolution across these viruses.

The rapid antigenic evolution of the 229E spike might seem puzzling given that coronaviruses have a lower mutation rate than other RNA viruses [21,22]. But the rate of phenotypic evolution is not equal to mutation rate; evolution also depends on the effects of mutations and how selection acts on them. These other factors explain why influenza undergoes rapid antigenic evolution while measles does not, despite having a similar mutation rate. Specifically, mutations to influenza hemagglutinin are often well tolerated [68], and single hemagglutinin mutations can have huge effects on escaping polyclonal sera [69]. In contrast, measles surface proteins are less tolerant of mutations [70], and the single mutations that are tolerated never more than modestly affect measles neutralization by polyclonal sera [71]. In these respects, coronaviruses unfortunately seem more similar to influenza than measles. The neutralizing antibody response to SARS-CoV-2 is often focused on just a small portion of spike [36,61,72,73], and key receptor-binding loops are mutationally tolerant in the spikes of both 229E [25,53] and SARS-CoV-2 [74]. Therefore, even though mutations to coronaviruses occur at a lower rate, they are acted on by selection in a fashion more similar to influenza than measles [27].

A striking aspect of our results is the extreme person-to-person variation in how rapidly neutralizing immunity is eroded by the evolution of coronavirus 229E. Some sera that potently

neutralize contemporaneous virus have no detectable activity against viral strains isolated 8 + years later. But other sera maintain neutralizing activity against strains isolated over two decades later. This finding is reminiscent of how mutations to influenza virus can have vastly different effects on neutralization by sera from different individuals [69]. Identifying what factors determine how rapidly an individual's coronavirus immunity is eroded by viral mutations is an important area for future work, as it would be desirable for SARS-CoV-2 vaccines to elicit immunity that is relatively robust to viral evolution.

The biggest question is what our work implies about possible antigenic evolution by SARS-CoV-2. While it is impossible to know if SARS-CoV-2 will evolve similarly to 229E, it is ominous that mutations affecting neutralization by polyclonal human sera are already present among SARS-CoV-2 lineages [54,59,61,73,75–77] even though a large fraction of the human population is still naive and so presumably exerting little immune pressure on the virus. But two facts provide hope even in light of our observation that human coronaviruses evolve to escape neutralizing immunity. First, the level of immunity required to prevent severe COVID-19 may be low [3], perhaps because the slower course of disease provides more time for a recall immune response than for "quicker" viruses such as influenza. An optimistic interpretation is that disease might often be mild even if viral antigenic evolution allows re-infections. Second, many leading SARS-CoV-2 vaccines use new technologies such as mRNA-based delivery [78] that should make it easy to update the vaccine if there is antigenic evolution in spike. For this reason, we suggest that SARS-CoV-2 evolution should be monitored for antigenic mutations that might make it advisable to periodically update vaccines.

Methods

Ethics statement

The human sera from the 1980s and 1990s from the Infectious Disease Sciences Biospecimen Repository at the Vaccine and Infectious Disease Division (VIDD) of the Fred Hutchinson Cancer Research Center were collected from prospective bone marrow donors with approval from the Fred Hutch's Human Subjects Institutional Review Board. The modern children's sera from 2020 are residual sera collected at Seattle Children's Hospital with approval from the Seattle Children's Hospital Human Subjects Institutional Review Board. All sera are fully de-identified.

Computer code

The computer code is on GitHub at https://github.com/jbloomlab/CoV_229E_antigenic_drift. Relevant parts of this GitHub repository are called out in the Methods below; in addition the repository itself includes a README that aids in navigation.

Phylogenetic analysis of 229E spikes

To assemble a set of 229E spikes, we downloaded all accessions for "Human coronavirus 229E (taxid:1137)" available from NCBI Virus as of July-13-2020. These accessions are listed at https://github.com/jbloomlab/CoV_229E_antigenic_drift/blob/master/data/NCBI_Virus_229E_accessions.csv. The NCBI information for some sequence accessions (particularly older sequences) were missing metadata that was available in publications describing the sequences [24,26]. For these accessions, we manually extracted the relevant metadata from the publications (see https://github.com/jbloomlab/CoV_229E_antigenic_drift/blob/master/data/extra_229E_accessions_metadata.yaml). We also identified a few sequences that were clear outliers on the date-to-tip regression in the analyses described below, and so are probably mis-

annotations; these accessions were excluded (see https://github.com/jbloomlab/CoV_229E_ antigenic_drift/blob/master/data/accessions_to_include_exclude_annotate.yaml).

We parsed full-length human-isolate spikes encoding unique proteins from this sequence set (see https://github.com/jbloomlab/CoV_229E_antigenic_drift/blob/master/results/get_ parse_spikes.md), used `mafft` [79] to align the protein sequences, and used a custom Python script (https://github.com/jbloomlab/CoV_229E_antigenic_drift/blob/master/prot_to_ codon_alignment.py) to build a codon alignment from the protein alignment (S1 Data). We used GARD [80,81] to screen for recombination (see tanglegram in S2 Fig and code at https:// github.com/jbloomlab/CoV_229E_antigenic_drift/blob/master/results/gard_tanglegram.md).

The phylogenetic tree topology was inferred using IQ-TREE [82] using a codon-substitution model [83] with a transition-transversion ratio and F3X4 empirical codon frequencies. We then used `TreeTime` [84] to root the tree (S2 Fig) and also re-scale the branch lengths for the time tree in Fig 1A. The tree images were rendered using ETE 3 [85].

To compute the variability at each site in spike (Fig 4A), we used the same alignment as for the phylogenetic analysis. We then computed the amino-acid variability at each site as the effective number of amino acids, which is the exponential of the Shannon entropy [86]. The domains of spike were annotated using the definitions in [53], which are provided at https:// github.com/jbloomlab/CoV_229E_antigenic_drift/blob/master/data/AAK32191_hand_ annotated.gp.

The Shannon entropy for each site was mapped onto the structure of 229E spike (pdb 6U7H) to produce Fig 4B. Pymol v 2.4.1 was used to visualize the structure. There are 3 gaps in this structure, including one in the NTD that included 2 variable sites which we were unable to include in the visualization.

Plasmids encoding 229E spikes and RBD chimeras

The protein sequences of the spikes used in the experiments are in S2 Data. We deleted the last 19 amino acids of the spike's C-terminus (in the cytoplasmic tail) as this modification has been reported [13,46,47] and validated in our hands (S3 Fig) to improve titers of virions pseudo-typed with spike. For the 1984, 1992, 2001, 2008, and 2016 spikes, the protein sequence matches the Genbank sequences for these viral strains (Fig 1A and S1 Data) except for the tail deletion. For the RBD chimeras, we annotated domains of spike as in [53]; see https://github. com/jbloomlab/CoV_229E_antigenic_drift/blob/master/data/AAK32191_hand_annotated. gp. We then designed the RBD-chimera proteins by replacing the RBD of the 1984 spike with the RBD of each of the 1992, 2001, 2008, and 2016 spikes.

We designed human-codon-optimized gene sequences encoding each of these spike proteins using the tool provided by Integrated DNA Technologies, had the genes synthesized commercially, and cloned them into a CMV-driven expression plasmid. Genbank sequences of the resulting plasmids are at https://github.com/jbloomlab/CoV_229E_antigenic_drift/tree/ master/exptl_data/plasmid_maps. The names of the plasmids are listed below (note how the names include "delta19" or "d19" to indicate the C-terminal deletion as well as the year for that viral strain and whether it is a chimera; note also that we created a plasmid for the 2016 spike that did not have the C-terminal deletion for the experiments in S3 Fig that validated the benefits of the deletion):

- HDM-229E-Spike-d19-1984

- HDM-229E-Spike-d19-1992

- HDM-229E-Spike-d19-2001

- HDM-229E-Spike-d19-2008

- HDM-229E-Spike-Seattle2016

- HDM-229E-Spike-delta19-Seattle2016

- HDM-229E-Spike-d19-1984-1992RBD

- HDM-229E-Spike-d19-1984-2001RBD

- HDM-229E-Spike-d19-1984-2008RBD

- HDM-229E-Spike-d19-1984-2016RBD

Generation and titering of 229E spike-pseudotyped lentiviral particles encoding luciferase and ZsGreen

We generated spike-pseudotyped lentiviral particles using the same approach that we have recently described for SARS-CoV-2 [13,87]. This approach involves creating pseudotyped lentiviral particles by transfecting cells with a plasmid expressing spike, a plasmid expressing a lentiviral backbone encoding luciferase and ZsGreen, and plasmids expressing the other lentiviral proteins necessary for virion formation [13,87]. The only modifications for this study are that we used the plasmids expressing the 229E spike described above rather than plasmids expressing the SARS-CoV-2 spike, and that after producing the pseudotyped lentiviral particles we infected them into target cells engineered to be infectable by the 229E spike.

Specifically, the 229E spike binds to human aminopeptidase N (APN) to initiate viral entry [33]. Therefore, to make 293T cells infectable by 229E, we transiently transfected them with an APN protein expression plasmid (SinoBiological, NM_001150.2) prior to seeding the cells for infection. To further promote lentiviral infection, we simultaneously transiently transfected them with a plasmid encoding transmembrane serine protease 2 (TMPRSS2), which facilitates 229E-spike mediated viral entry by cleaving and activating the spike [48]. We used the TMPRSS2-expressing plasmid pHAGE2_EF1aInt_TMPRSS2_IRES_mCherry [88].

For titering the spike-pseudotyped particles in these cells, we used the following procedure. To mitigate any possible well-to-well differences in transfection efficiency in a 96-well plate format, we first bulk transfected a dish of 293T cells, followed by seeding the 96-well plates routinely used in neutralization assays and viral titering. Specifically, an approximately 90% confluent 10 cm dish of 293T cells was transfected with 8.5 μg APN-expressing plasmid, 1 μg of TMPRSS2-expressing plasmid, and 0.5 μg of carrier DNA (Promega, E4881) to achieve an 8.5:1 ratio of APN:TMPRSS2. We found that this ratio gave sufficient TMPRSS2 expression, while maintaining low levels of cell toxicity. Cells were transfected using the Bioland Scientific BioT transfection reagent following the manufacturer's protocol but incubating transfection complexes for 15 minutes at room temperature instead of the recommended 5 minutes as we have anecdotally observed that this extended incubation increases transfection efficiency. After 5–6 hours, transfection supernatant was removed and the APN and TMPRSS2-transfected 293T cells were trypsinized (Fisher, MT25053CI). Cells were then seeded in clear bottom, black-walled, poly-L-lysine coated 96-well plates that were either professionally pre-coated (Greiner, 655936) or hand-coated (Greiner, 655090) with poly-L-lysine solution (Millipore Sigma, P4704) at 1.75x10e4 cells per well in 50 μL D10 growth media (DMEM with 10% heat-inactivated FBS, 2 mM L-glutamine, 100 U/mL penicillin, and 100 μg/mL streptomycin). Plates were incubated at 37˚C with 5% CO_2 for 20–24 hours, and cells were infected with serial 2-fold serial dilutions of the pseudotyped lentiviral particles. These viral dilutions were made in TC-treated "set-up" 96-well plates and then transferred to the pre-seeded 293T-ACE2-TMPRSS2 cells from the previous day.

Approximately 50–52 hours later, we quantified infection by reading the luminescence signal produced from the luciferase encoded in the lentiviral backbone. Specifically, 100 μL of media in each well was removed—while being sure to leave the cells undisturbed—leaving approximately 30 μL of media left over. Then an equal volume of Bright-Glo reagent (Promega, E2610) was added to the remaining 30 uL of media in each well and the solution was mixed up and down to ensure complete cell lysis. In order to minimize the potential for premature luciferase excitation, special care was taken to protect the assay plates from light. Mainly, assay plate preparation was performed in a biosafety hood with the lights off and plates were covered in tin foil after the addition of the luciferase reagent. The luminescence was then measured on a TECAN Infinite M1000 Pro plate reader with no attenuation and a luminescence integration time of 1 second. S3 Fig shows the titers achieved for each 229E spike variant, and also demonstrates the importance of the spike cytoplasmic tail deletion and the expression of APN and TMPRSS2 for efficient viral infection. Note that for one panel in S3 Fig, we instead determined the titer by using flow cytometry to detect the fraction of cells expressing the ZsGreen also encoded in the lentiviral backbone.

Human sera

All sera used in this study, along with relevant metadata (e.g., collection date, patient age, and the measured neutralization titer against each assayed virus) are listed in S3 Data, which is also available at https://github.com/jbloomlab/CoV_229E_antigenic_drift/blob/master/exptl_data/results/all_neut_titers.csv.

Most of the historical human sera from the 1980s and 1990s are identified by the prefix SD in S3 Data (e.g., SD85_1). These sera were obtained from the Infectious Disease Sciences Biospecimen Repository at the Vaccine and Infectious Disease Division (VIDD) of the Fred Hutchinson Cancer Research Center in Seattle, WA, and were collected from prospective bone marrow donors with approval from the Human Subjects Institutional Review Board. A few of the historical sera are residual samples obtained from Bloodworks Northwest that were collected from adults in Seattle; these sera are identified by the prefix FH in S3 Data (e.g., FH007TR). A few of the sera were collected from subjects with exact ages that were unknown, but were adults old enough to have been alive in 1984 (the isolation year of the first spike in our panel). No information on recent respiratory virus infections was available for any of the sera samples.

The modern children's sera from 2020 are identified by the prefix POP_ in S3 Data (e.g., POP_0007), and are residual sera collected at Seattle Children's Hospital in Seattle, WA, in March of 2020 with approval from the Human Subjects Institutional Review Board. Each of these serum samples is from a unique individual who was confirmed to be seronegative for SARS-CoV-2 by an anti-RBD ELISA [89].

The modern adult sera from 2020 are identified by the prefix AUSAB (e.g., AUSAB-01) in S3 Data, and are residual sera from University of Washington Lab Medicine that were collected for testing for HBsAb (for which they tested negative).

For a negative control, we used serum from a goat that had not been infected with the 229E human coronavirus; namely WHO goat serum (FR-1377) procured from the International Reagent Resource.

All sera were heat inactivated prior to use by incubation at 56°C for approximately 30 minutes.

Neutralization assays

The 293T cells used for our neutralization assays were transfected to express APN and TMPRSS2 and seeded as for the viral titering described above. The neutralization assays were

set up at 20–24 hours after seeding of the cells into 96-well plates. First, the heat-inactivated serum samples were diluted 1:10 in D10 growth media followed by 3-fold serial dilutions in TC-coated 96-well "set-up" plates, ultimately giving seven total dilutions per sample. These dilutions were done in duplicate for each serum sample. Each 229E spike-pseudotyped lentivirus was then diluted to achieve luciferase readings of approximately 200,000 RLUs per well (the exact dilution factor varied among viruses due to differences in titers; see S3 Fig). An equal volume of virus was then added to each well of the virus plus sera "set-up" plates, and these plates were incubated for 1 hour at 37˚C with 5% CO_2, after which 100 uL of each virus plus sera mixture were transferred to the 293T-APN-TMPRSS2 cell plate that had been seeded the day prior. Plates were incubated at 37˚C with 5% CO_2 for approximately 50–52 hours, and then the luciferase signal was read as described above for viral titering.

Each neutralization plate contained a column of positive control wells consisting of cells plus virus incubated with D10 media but no sera, and a negative control consisting of virus but no cells (we also confirmed that using a cells-only negative control gave similar results). The fraction infectivity was computed at each serum dilution as the fraction of the signal for the positive control (averaged across the two positive control wells for each row) after subtracting the background reading for the negative control. We then fit 2-parameter Hill curves with baselines fixed to 1 and 0 using neutcurve (https://jbloomlab.github.io/neutcurve/). Note that the serum concentration reported in these curves is the concentration at which the virus was pre-incubated with the sera for 1 hour. All of the neutralization curves are plotted in S4 Fig. All of the IC50s are tabulated in S3 Data. See https://github.com/jbloomlab/CoV_229E_ antigenic_drift/tree/master/exptl_data for raw and processed plate reader data and all of the computer code used for the fitting. Note that all assays were done in duplicate, but some sera-virus pairs have additional readings as we re-ran selected sera-virus pairs to confirm that results remained consistent across different assay days. In all cases the day-to-day consistency was good, and the reported values are the mean IC50s across all assays.

Supporting information

S1 Fig. The evolution of the 229E spike is clock-like, with the number of substitutions per site proportional to time. (A) Phylogenetic tree exactly like that in Fig 1 but with branch lengths proportional to divergence (not re-scaled based on tip isolation date). (B) A plot produced by TreeTime showing the correlation between the distance of tip nodes from the root and sampling date. The fact that all points fall on a line indicates that the evolution is clock-like.
(TIF)

S2 Fig. Although there is some evidence of recombination among closely related 229E spikes, this recombination does not alter the relative phylogenetic relationships among the spikes used in the experiments. Specifically, GARD was used to analyze the same set of 229E spike sequences used in Fig 1 with a nucleotide substitution model and three gamma-distributed rate classes. The best-fitting model had a single recombination breakpoint at nucleotide 1089 that improved the AIC by 60 units. The trees for each partition were then rooted and branch-re-scaled using TreeTime, and the resulting tanglegram was rendered using dendextend. As can be seen above, the recombination is all between closely related sequences and does not alter the relative position of the 1984, 1992, 2001, 2008, and 2016 spikes used in the experiments. See https://github.com/jbloomlab/CoV_229E_antigenic_drift/blob/master/ results/gard_tanglegram.md for details of the analysis steps described above.
(TIF)

S3 Fig. The 229E spikes with a cytoplasmic tail deletion pseudotype lentiviral particles that efficiently infect 293T cells expressing the spike's receptor aminopeptidase N (APN) and the activating protease TMPRSS2. (A) Titer in transduction units per ml as determined using flow cytometry of lentiviral particles pseudotyped with the full-length 2016 spike or that spike with a deletion of the last 19 residues in spike (the end of the cytoplasmic tail) on 293T cells transfected with a plasmid expressing APN. The dotted gray line is the limit of detection, and the titers in the absence of spike were below this line (undetectable). (B) Efficient entry by the pseudotyped virions depends on expression of APN and to a lesser extent TMPRSS2. Virions pseudotyped with the 2016 spike with the C-terminal deletion were infected into 293T cells transfected with plasmids expressing one or both of APN and TMPRSS2, and titers were determined by luciferase luminescence. Titers are normalized to one. (C) All of the 229E spikes and chimeras used in this study mediated efficient viral entry. Lentiviral particles were pseudotyped with the indicated spike (in all cases with the C-terminal deletion) and titers were determined using luciferase luminescence on 293T cells transfected with plasmids expressing APN and TMPRSS2.
(TIF)

S4 Fig. Neutralization curves for all assays. Each facet is a serum, with titles indicating the year the serum was collected. Each point is the fraction infectivity at that serum concentration averaged across at least two replicates (error bars are standard error), with colors indicating the virus. The fits are 2-parameter Hill curves with baselines fixed to 1 and 0, and were fit using neutcurve (https://jbloomlab.github.io/neutcurve/). IC50s are in S3 Data. The curves are also at https://github.com/jbloomlab/CoV_229E_antigenic_drift/blob/master/exptl_data/results/all_neut_by_sera.pdf
(TIF)

S5 Fig. Initial screening of sera to identify samples with neutralizing titers of at least 1:90 that were then used for the rest of the studies described in the paper. Each sera was tested against the most-recent virus isolated prior to the serum collection date: in other words, sera collected between 1985–1990 was tested against the 1984 spike, sera collected between 1992–1995 was tested against the 1992 spike, and sera collected in 2020 was tested against the 2016 spike. Each point shows the neutralizing titer for a different serum (see S4 Fig for full neutralization curves). Sera above the cutoff of 1:90 (blue dashed line) was then used for further studies against the full panel of viruses (e.g., Figs 2, 3, and 4). The numbers at the top of the plot indicate the number of sera above the cutoff out of the total sera tested in each timeframe. The dotted horizontal line at the bottom of the plot is the lower limit of detection of the neutralization assay. Quantitative neutralization titers for each sera are in S3 Data.
(TIF)

S1 Data. Codon-level alignment of the 229E spike sequences. This FASTA alignment is at https://github.com/jbloomlab/CoV_229E_antigenic_drift/blob/master/results/spikes_aligned_codon.fasta
(TXT)

S2 Data. A ZIP of GenPept files giving the protein sequences of the spikes used in the experiments. There are nine sequences: the five spikes from the 1984, 1992, 2001, 2008, and 2016 viruses (named by strain as shown in Fig 1A), and the four chimeras that consist of the 1984 spike with the RBD of each of the other strains. Each GenPept file annotates key domains in the spike. Note that the C-terminal 19 amino acids are deleted off each spike. These files are at https://github.com/jbloomlab/CoV_229E_antigenic_drift/tree/master/results/seqs_for_

expts
(ZIP)

S3 Data. A CSV file giving the neutralization titer, collection date, and subject age at time of collection date for each serum sample analyzed in this study. This file is at https://github.com/jbloomlab/CoV_229E_antigenic_drift/blob/master/exptl_data/results/all_neut_titers.csv
(CSV)

Acknowledgments

We thank David Veesler, Allison Greaney, Tyler Starr, Kathryn Kistler, and Trevor Bedford for helpful comments. We also thank the Vaccine and Infectious Diseases Division of the Fred Hutch for supporting the biorepository used for the 1980s and 1990s sera.

Author Contributions

Conceptualization: Rachel T. Eguia, Katharine H. D. Crawford, Jesse D. Bloom.

Data curation: Terry Stevens-Ayers, Alexander L. Greninger, Janet A. Englund, Michael J. Boeckh.

Funding acquisition: Jesse D. Bloom.

Investigation: Rachel T. Eguia, Laurel Kelnhofer-Millevolte.

Methodology: Rachel T. Eguia, Katharine H. D. Crawford.

Resources: Terry Stevens-Ayers, Alexander L. Greninger, Janet A. Englund, Michael J. Boeckh.

Software: Katharine H. D. Crawford, Jesse D. Bloom.

Supervision: Jesse D. Bloom.

Visualization: Jesse D. Bloom.

Writing – original draft: Rachel T. Eguia, Jesse D. Bloom.

Writing – review & editing: Katharine H. D. Crawford, Terry Stevens-Ayers, Alexander L. Greninger, Janet A. Englund, Michael J. Boeckh, Jesse D. Bloom.

References

1. Addetia A, Crawford KHD, Dingens A, Zhu H, Roychoudhury P, Huang M-L, et al. Neutralizing Antibodies Correlate with Protection from SARS-CoV-2 in Humans during a Fishery Vessel Outbreak with a High Attack Rate. J Clin Microbiol. 2020; 58. https://doi.org/10.1128/JCM.02107-20 PMID: 32826322

2. Lumley SF, O'Donnell D, Stoesser NE, Matthews PC, Howarth A, Hatch SB, et al. Antibody Status and Incidence of SARS-CoV-2 Infection in Health Care Workers. N Engl J Med. 2021; 384: 533–540. https://doi.org/10.1056/NEJMoa2034545 PMID: 33369366

3. Polack FP, Thomas SJ, Kitchin N, Absalon J, Gurtman A, Lockhart S, et al. Safety and Efficacy of the BNT162b2 mRNA Covid-19 Vaccine. N Engl J Med. 2020;0: null. https://doi.org/10.1056/NEJMoa2034577 PMID: 33301246

4. Alsoussi WB, Turner JS, Case JB, Zhao H, Schmitz AJ, Zhou JQ, et al. A Potently Neutralizing Antibody Protects Mice against SARS-CoV-2 Infection. J Immunol. 2020; 205: 915–922. https://doi.org/10.4049/jimmunol.2000583 PMID: 32591393

5. McMahan K, Yu J, Mercado NB, Loos C, Tostanoski LH, Chandrashekar A, et al. Correlates of protection against SARS-CoV-2 in rhesus macaques. Nature. 2020; 1–8. https://doi.org/10.1038/s41586-020-03041-6 PMID: 33276369

6. Walls AC, Park Y-J, Tortorici MA, Wall A, McGuire AT, Veesler D. Structure, Function, and Antigenicity of the SARS-CoV-2 Spike Glycoprotein. Cell. 2020; 181: 281–292.e6. https://doi.org/10.1016/j.cell.2020.02.058 PMID: 32155444

7. Zost SJ, Gilchuk P, Case JB, Binshtein E, Chen RE, Nkolola JP, et al. Potently neutralizing and protective human antibodies against SARS-CoV-2. Nature. 2020; 584: 443–449. https://doi.org/10.1038/s41586-020-2548-6 PMID: 32668443

8. Edridge AWD, Kaczorowska J, Hoste ACR, Bakker M, Klein M, Loens K, et al. Seasonal coronavirus protective immunity is short-lasting. Nat Med. 2020; 26: 1691–1693. https://doi.org/10.1038/s41591-020-1083-1 PMID: 32929268

9. Hendley JO, Fishburne HB, Jack M. Gwaltney J. Coronavirus Infections in Working Adults. Am Rev Respir Dis. 1972; 105: 805–811. https://doi.org/10.1164/arrd.1972.105.5.805 PMID: 5020629

10. Schmidt OW, Allan ID, Cooney MK, Foy HM, Fox JP. Rises in titers of antibody to human corona viruses OC43 and 229E in Seattle families during 1975–1979. Am J Epidemiol. 1986; 123: 862–868. https://doi.org/10.1093/oxfordjournals.aje.a114315 PMID: 3008551

11. Aldridge RW, Lewer D, Beale S, Johnson AM, Zambon M, Hayward AC, et al. Seasonality and immunity to laboratory-confirmed seasonal coronaviruses (HCoV-NL63, HCoV-OC43, and HCoV-229E): results from the Flu Watch cohort study. Wellcome Open Res. 2020; 5: 52. https://doi.org/10.12688/wellcomeopenres.15812.2 PMID: 33447664

12. Ibarrondo FJ, Fulcher JA, Goodman-Meza D, Elliott J, Hofmann C, Hausner MA, et al. Rapid Decay of Anti–SARS-CoV-2 Antibodies in Persons with Mild Covid-19. N Engl J Med. 2020; 383: 1085–1087. https://doi.org/10.1056/NEJMc2025179 PMID: 32706954

13. Crawford KHD, Dingens AS, Eguia R, Wolf CR, Wilcox N, Logue JK, et al. Dynamics of neutralizing antibody titers in the months after SARS-CoV-2 infection. J Infect Dis. 2020; 223: 197–205. https://doi.org/10.1093/infdis/jiaa618 PMID: 33000143

14. Gaebler C, Wang Z, Lorenzi JCC, Muecksch F, Finkin S, Tokuyama M, et al. Evolution of Antibody Immunity to SARS-CoV-2. Nature. 2021. https://doi.org/10.1038/s41586-021-03207-w PMID: 33461210

15. Rodda LB, Netland J, Shehata L, Pruner KB, Morawski PA, Thouvenel CD, et al. Functional SARS-CoV-2-specific immune memory persists after mild COVID-19. Cell. 2020 [cited 8 Dec 2020]. https://doi.org/10.1016/j.cell.2020.11.029 PMID: 33296701

16. Wajnberg A, Amanat F, Firpo A, Altman DR, Bailey MJ, Mansour M, et al. Robust neutralizing antibodies to SARS-CoV-2 infection persist for months. Science. 2020; 370: 1227–1230. https://doi.org/10.1126/science.abd7728 PMID: 33115920

17. Couch RB, Kasel JA. Immunity to influenza in man. Annu Rev Microbiol. 1983; 37: 529–549. https://doi.org/10.1146/annurev.mi.37.100183.002525 PMID: 6357060

18. Yu X, Tsibane T, McGraw PA, House FS, Keefer CJ, Hicar MD, et al. Neutralizing antibodies derived from the B cells of 1918 influenza pandemic survivors. Nature. 2008; 455: 532–536. https://doi.org/10.1038/nature07231 PMID: 18716625

19. Bedford T, Suchard MA, Lemey P, Dudas G, Gregory V, Hay AJ, et al. Integrating influenza antigenic dynamics with molecular evolution. eLife. 2014; 3: e01914. https://doi.org/10.7554/eLife.01914 PMID: 24497547

20. Ranjeva S, Subramanian R, Fang VJ, Leung GM, Ip DKM, Perera RAPM, et al. Age-specific differences in the dynamics of protective immunity to influenza. Nat Commun. 2019; 10: 1660. https://doi.org/10.1038/s41467-019-09652-6 PMID: 30971703

21. Denison MR, Graham RL, Donaldson EF, Eckerle LD, Baric RS. Coronaviruses. RNA Biol. 2011; 8: 270–279. https://doi.org/10.4161/rna.8.2.15013 PMID: 21593585

22. Sanjuán R, Nebot MR, Chirico N, Mansky LM, Belshaw R. Viral Mutation Rates. J Virol. 2010; 84: 9733–9748. https://doi.org/10.1128/JVI.00694-10 PMID: 20660197

23. Reed SE. The behaviour of recent isolates of human respiratory coronavirus in vitro and in volunteers: Evidence of heterogeneity among 229E-related strains. J Med Virol. 1984; 13: 179–192. https://doi.org/10.1002/jmv.1890130208 PMID: 6319590

24. Shirato K, Kawase M, Watanabe O, Hirokawa C, Matsuyama S, Nishimura H, et al. Differences in neutralizing antigenicity between laboratory and clinical isolates of HCoV-229E isolated in Japan in 2004–2008 depend on the S1 region sequence of the spike protein. J Gen Virol. 2012; 93: 1908–1917. https://doi.org/10.1099/vir.0.043117-0 PMID: 22673931

25. Wong AHM, Tomlinson ACA, Zhou D, Satkunarajah M, Chen K, Sharon C, et al. Receptor-binding loops in alphacoronavirus adaptation and evolution. Nat Commun. 2017; 8: 1735. https://doi.org/10.1038/s41467-017-01706-x PMID: 29170370

26. Chibo D, Birch C. Analysis of human coronavirus 229E spike and nucleoprotein genes demonstrates genetic drift between chronologically distinct strains. J Gen Virol. 2006; 87: 1203–1208. https://doi.org/10.1099/vir.0.81662-0 PMID: 16603522

27. Kistler KE, Bedford T. Evidence for adaptive evolution in the receptor-binding domain of seasonal coronaviruses. eLife. 2021; 10: e64509. https://doi.org/10.7554/eLife.64509 PMID: 33463525

28. Ren L, Zhang Y, Li J, Xiao Y, Zhang J, Wang Y, et al. Genetic drift of human coronavirus OC43 spike gene during adaptive evolution. Sci Rep. 2015; 5: 11451. https://doi.org/10.1038/srep11451 PMID: 26099036

29. Tortorici MA, Veesler D. Structural insights into coronavirus entry. Adv Virus Res. 2019; 105: 93–116. https://doi.org/10.1016/bs.aivir.2019.08.002 PMID: 31522710

30. Callow KA. Effect of specific humoral immunity and some non-specific factors on resistance of volunteers to respiratory coronavirus infection. J Hyg (Lond). 1985; 95: 173–189. https://doi.org/10.1017/s0022172400062410 PMID: 2991366

31. Callow KA, Parry HF, Sergeant M, Tyrrell DA. The time course of the immune response to experimental coronavirus infection of man. Epidemiol Infect. 1990; 105: 435–446. https://doi.org/10.1017/s0950268800048019 PMID: 2170159

32. Hofmann H, Pyrc K, van der Hoek L, Geier M, Berkhout B, Pöhlmann S. Human coronavirus NL63 employs the severe acute respiratory syndrome coronavirus receptor for cellular entry. Proc Natl Acad Sci U S A. 2005; 102: 7988–7993. https://doi.org/10.1073/pnas.0409465102 PMID: 15897467

33. Yeager CL, Ashmun RA, Williams RK, Cardellichio CB, Shapiro LH, Look AT, et al. Human aminopeptidase N is a receptor for human coronavirus 229E. Nature. 1992; 357: 420–422. https://doi.org/10.1038/357420a0 PMID: 1350662

34. Hulswit RJG, Lang Y, Bakkers MJG, Li W, Li Z, Schouten A, et al. Human coronaviruses OC43 and HKU1 bind to 9-O-acetylated sialic acids via a conserved receptor-binding site in spike protein domain A. Proc Natl Acad Sci U S A. 2019; 116: 2681–2690. https://doi.org/10.1073/pnas.1809667116 PMID: 30679277

35. Abe KT, Li Z, Samson R, Samavarchi-Tehrani P, Valcourt EJ, Wood H, et al. A simple protein-based surrogate neutralization assay for SARS-CoV-2. JCI Insight. 5. https://doi.org/10.1172/jci.insight.142362 PMID: 32870820

36. Piccoli L, Park Y-J, Tortorici MA, Czudnochowski N, Walls AC, Beltramello M, et al. Mapping Neutralizing and Immunodominant Sites on the SARS-CoV-2 Spike Receptor-Binding Domain by Structure-Guided High-Resolution Serology. Cell. 2020; 183: 1024–1042.e21. https://doi.org/10.1016/j.cell.2020.09.037 PMID: 32991844

37. Tan CW, Chia WN, Qin X, Liu P, Chen MI-C, Tiu C, et al. A SARS-CoV-2 surrogate virus neutralization test based on antibody-mediated blockage of ACE2–spike protein–protein interaction. Nat Biotechnol. 2020; 38: 1073–1078. https://doi.org/10.1038/s41587-020-0631-z PMID: 32704169

38. Hamre D, Procknow JJ. A New Virus Isolated from the Human Respiratory Tract. Proc Soc Exp Biol Med. 1966; 121: 190–193. https://doi.org/10.3181/00379727-121-30734 PMID: 4285768

39. van der Hoek L, Pyrc K, Jebbink MF, Vermeulen-Oost W, Berkhout RJM, Wolthers KC, et al. Identification of a new human coronavirus. Nat Med. 2004; 10: 368–373. https://doi.org/10.1038/nm1024 PMID: 15034574

40. Hodcroft EB. Seasonal CoV and SARS CoV live full-genome builds. In: Virological [Internet]. 2020 [cited 10 Dec 2020]. Available: https://virological.org/t/seasonal-cov-sars-cov-live-full-genome-builds

41. Bedford T, Cobey S, Pascual M. Strength and tempo of selection revealed in viral gene genealogies. BMC Evol Biol. 2011; 11: 220. https://doi.org/10.1186/1471-2148-11-220 PMID: 21787390

42. Fitch WM, Bush RM, Bender CA, Cox NJ. Long term trends in the evolution of H(3) HA1 human influenza type A. Proc Natl Acad Sci U S A. 1997; 94: 7712–7718. https://doi.org/10.1073/pnas.94.15.7712 PMID: 9223253

43. Grenfell BT, Pybus OG, Gog JR, Wood JLN, Daly JM, Mumford JA, et al. Unifying the Epidemiological and Evolutionary Dynamics of Pathogens. Science. 2004; 303: 327–332. https://doi.org/10.1126/science.1090727 PMID: 14726583

44. Lemey P, Rambaut A, Bedford T, Faria N, Bielejec F, Baele G, et al. Unifying Viral Genetics and Human Transportation Data to Predict the Global Transmission Dynamics of Human Influenza H3N2. PLOS Pathog. 2014; 10: e1003932. https://doi.org/10.1371/journal.ppat.1003932 PMID: 24586153

45. Nelson MI, Simonsen L, Viboud C, Miller MA, Holmes EC. Phylogenetic Analysis Reveals the Global Migration of Seasonal Influenza A Viruses. PLOS Pathog. 2007; 3: e131. https://doi.org/10.1371/journal.ppat.0030131 PMID: 17941707

46. Kawase M, Shirato K, Matsuyama S, Taguchi F. Protease-Mediated Entry via the Endosome of Human Coronavirus 229E. J Virol. 2009; 83: 712–721. https://doi.org/10.1128/JVI.01933-08 PMID: 18971274

47. Rogers TF, Zhao F, Huang D, Beutler N, Burns A, He W, et al. Isolation of potent SARS-CoV-2 neutralizing antibodies and protection from disease in a small animal model. Science. 2020; 369: 956–963. https://doi.org/10.1126/science.abc7520 PMID: 32540903

48. Bertram S, Dijkman R, Habjan M, Heurich A, Gierer S, Glowacka I, et al. TMPRSS2 Activates the Human Coronavirus 229E for Cathepsin-Independent Host Cell Entry and Is Expressed in Viral Target Cells in the Respiratory Epithelium. J Virol. 2013; 87: 6150–6160. https://doi.org/10.1128/JVI.03372-12 PMID: 23536651

49. Widge AT, Rouphael NG, Jackson LA, Anderson EJ, Roberts PC, Makhene M, et al. Durability of Responses after SARS-CoV-2 mRNA-1273 Vaccination. N Engl J Med. 2020 [cited 10 Dec 2020]. https://doi.org/10.1056/NEJMc2032195 PMID: 33270381

50. Sandbulte MR, Westgeest KB, Gao J, Xu X, Klimov AI, Russell CA, et al. Discordant antigenic drift of neuraminidase and hemagglutinin in H1N1 and H3N2 influenza viruses. Proc Natl Acad Sci. 2011; 108: 20748–20753. https://doi.org/10.1073/pnas.1113801108 PMID: 22143798

51. Underwood PA. Serology and Energetics of Cross-Reactions Among the H3 Antigens of Influenza Viruses. Infect Immun. 1980; 27: 397–404. https://doi.org/10.1128/IAI.27.2.397-404.1980 PMID: 6155332

52. Liò P, Goldman N. Phylogenomics and bioinformatics of SARS-CoV. Trends Microbiol. 2004; 12: 106–111. https://doi.org/10.1016/j.tim.2004.01.005 PMID: 15058277

53. Li Z, Tomlinson AC, Wong AH, Zhou D, Desforges M, Talbot PJ, et al. The human coronavirus HCoV-229E S-protein structure and receptor binding. Bjorkman PJ, Boudker O, editors. eLife. 2019; 8: e51230. https://doi.org/10.7554/eLife.51230 PMID: 31650956

54. Greaney AJ, Loes AN, Crawford KHD, Starr TN, Malone KD, Chu HY, et al. Comprehensive mapping of mutations in the SARS-CoV-2 receptor-binding domain that affect recognition by polyclonal human plasma antibodies. Cell Host Microbe. 2021 [cited 16 Feb 2021]. https://doi.org/10.1016/j.chom.2021.02.003 PMID: 33592168

55. Chi X, Yan R, Zhang J, Zhang G, Zhang Y, Hao M, et al. A neutralizing human antibody binds to the N-terminal domain of the Spike protein of SARS-CoV-2. Science. 2020; 369: 650–655. https://doi.org/10.1126/science.abc6952 PMID: 32571838

56. Kemp SA, Collier DA, Datir R, Gayed S, Jahun A, Hosmillo M, et al. Neutralising antibodies drive Spike mediated SARS-CoV-2 evasion. medRxiv. 2020; 2020.12.05.20241927. https://doi.org/10.1101/2020.12.05.20241927 PMID: 33398302

57. Liu L, Wang P, Nair MS, Yu J, Rapp M, Wang Q, et al. Potent neutralizing antibodies against multiple epitopes on SARS-CoV-2 spike. Nature. 2020; 584: 450–456. https://doi.org/10.1038/s41586-020-2571-7 PMID: 32698192

58. McCallum M, Marco AD, Lempp F, Tortorici MA, Pinto D, Walls AC, et al. N-terminal domain antigenic mapping reveals a site of vulnerability for SARS-CoV-2. bioRxiv. 2021; 2021.01.14.426475. https://doi.org/10.1101/2021.01.14.426475 PMID: 33469588

59. McCarthy KR, Rennick LJ, Nambulli S, Robinson-McCarthy LR, Bain WG, Haidar G, et al. Natural deletions in the SARS-CoV-2 spike glycoprotein drive antibody escape. Science. 2021;eabf6950. https://doi.org/10.1126/science.abf6950 PMID: 33536258

60. Suryadevara N, Shrihari S, Gilchuk P, VanBlargan LA, Binshtein E, Zost SJ, et al. Neutralizing and protective human monoclonal antibodies recognizing the N-terminal domain of the SARS-CoV-2 spike protein. bioRxiv. 2021; 2021.01.19.427324. https://doi.org/10.1101/2021.01.19.427324 PMID: 33501445

61. Weisblum Y, Schmidt F, Zhang F, DaSilva J, Poston D, Lorenzi JC, et al. Escape from neutralizing antibodies by SARS-CoV-2 spike protein variants. Marsh M, van der Meer JW, Montefiore D, editors. eLife. 2020; 9: e61312. https://doi.org/10.7554/eLife.61312 PMID: 33112236

62. Zhou H, Chen Y, Zhang S, Niu P, Qin K, Jia W, et al. Structural definition of a neutralization epitope on the N-terminal domain of MERS-CoV spike glycoprotein. Nat Commun. 2019; 10: 3068. https://doi.org/10.1038/s41467-019-10897-4 PMID: 31296843

63. Smith DJ, Lapedes AS, Jong JC de, Bestebroer TM, Rimmelzwaan GF, Osterhaus ADME, et al. Mapping the Antigenic and Genetic Evolution of Influenza Virus. Science. 2004; 305: 371–376. https://doi.org/10.1126/science.1097211 PMID: 15218094

64. Neher RA, Bedford T, Daniels RS, Russell CA, Shraiman BI. Prediction, dynamics, and visualization of antigenic phenotypes of seasonal influenza viruses. Proc Natl Acad Sci. 2016; 113: E1701–E1709. https://doi.org/10.1073/pnas.1525578113 PMID: 26951657

65. Fonville JM, Wilks SH, James SL, Fox A, Ventresca M, Aban M, et al. Antibody landscapes after influenza virus infection or vaccination. Science. 2014; 346: 996–1000. https://doi.org/10.1126/science.1256427 PMID: 25414313

66. Fonville JM, Fraaij PLA, de Mutsert G, Wilks SH, van Beek R, Fouchier RAM, et al. Antigenic Maps of Influenza A(H3N2) Produced With Human Antisera Obtained After Primary Infection. J Infect Dis. 2016; 213: 31–38. https://doi.org/10.1093/infdis/jiv367 PMID: 26142433

67. Li Y, Myers JL, Bostick DL, Sullivan CB, Madara J, Linderman SL, et al. Immune history shapes specificity of pandemic H1N1 influenza antibody responses. J Exp Med. 2013; 210: 1493–1500. https://doi.org/10.1084/jem.20130212 PMID: 23857983

68. Thyagarajan B, Bloom JD. The inherent mutational tolerance and antigenic evolvability of influenza hemagglutinin. Pascual M, editor. eLife. 2014; 3: e03300. https://doi.org/10.7554/eLife.03300 PMID: 25006036

69. Lee JM, Eguia R, Zost SJ, Choudhary S, Wilson PC, Bedford T, et al. Mapping person-to-person variation in viral mutations that escape polyclonal serum targeting influenza hemagglutinin. Lipsitch M, Kirkegaard K, Lipsitch M, editors. eLife. 2019; 8: e49324. https://doi.org/10.7554/eLife.49324 PMID: 31452511

70. Fulton BO, Sachs D, Beaty SM, Won ST, Lee B, Palese P, et al. Mutational Analysis of Measles Virus Suggests Constraints on Antigenic Variation of the Glycoproteins. Cell Rep. 2015; 11: 1331–1338. https://doi.org/10.1016/j.celrep.2015.04.054 PMID: 26004185

71. Muñoz-Alía MÁ, Nace RA, Zhang L, Russell SJ. Pathogenic measles viruses cannot evolve to bypass vaccine-induced neutralizing antibodies. bioRxiv. 2020; 2020.10.22.351189. https://doi.org/10.1101/2020.10.22.351189

72. Barnes CO, West AP, Huey-Tubman KE, Hoffmann MAG, Sharaf NG, Hoffman PR, et al. Structures of Human Antibodies Bound to SARS-CoV-2 Spike Reveal Common Epitopes and Recurrent Features of Antibodies. Cell. 2020; 182: 828–842.e16. https://doi.org/10.1016/j.cell.2020.06.025 PMID: 32645326

73. Liu Z, VanBlargan LA, Rothlauf PW, Bloyet L-M, Chen RE, Stumpf S, et al. Landscape analysis of escape variants identifies SARS-CoV-2 spike mutations that attenuate monoclonal and serum antibody neutralization. bioRxiv. 2020; 2020.11.06.372037. https://doi.org/10.1101/2020.11.06.372037 PMID: 33442690

74. Starr TN, Greaney AJ, Hilton SK, Ellis D, Crawford KHD, Dingens AS, et al. Deep Mutational Scanning of SARS-CoV-2 Receptor Binding Domain Reveals Constraints on Folding and ACE2 Binding. Cell. 2020; 182: 1295–1310.e20. https://doi.org/10.1016/j.cell.2020.08.012 PMID: 32841599

75. Cele S, Gazy I, Jackson L, Hwa S-H, Tegally H, Lustig G, et al. Escape of SARS-CoV-2 501Y.V2 variants from neutralization by convalescent plasma. medRxiv. 2021; 2021.01.26.21250224. https://doi.org/10.1101/2021.01.26.21250224

76. Wang Z, Schmidt F, Weisblum Y, Muecksch F, Barnes CO, Finkin S, et al. mRNA vaccine-elicited antibodies to SARS-CoV-2 and circulating variants. bioRxiv. 2021; 2021.01.15.426911. https://doi.org/10.1101/2021.01.15.426911 PMID: 33501451

77. Wibmer CK, Ayres F, Hermanus T, Madzivhandila M, Kgagudi P, Lambson BE, et al. SARS-CoV-2 501Y.V2 escapes neutralization by South African COVID-19 donor plasma. bioRxiv. 2021; 2021.01.18.427166. https://doi.org/10.1101/2021.01.18.427166 PMID: 33501446

78. Krammer F. SARS-CoV-2 vaccines in development. Nature. 2020; 586: 516–527. https://doi.org/10.1038/s41586-020-2798-3 PMID: 32967006

79. Katoh K, Standley DM. MAFFT Multiple Sequence Alignment Software Version 7: Improvements in Performance and Usability. Mol Biol Evol. 2013; 30: 772–780. https://doi.org/10.1093/molbev/mst010 PMID: 23329690

80. Kosakovsky Pond SL, Posada D, Gravenor MB, Woelk CH, Frost SDW. GARD: a genetic algorithm for recombination detection. Bioinformatics. 2006; 22: 3096–3098. https://doi.org/10.1093/bioinformatics/btl474 PMID: 17110367

81. Spielman SJ, Weaver S, Shank SD, Magalis BR, Li M, Kosakovsky Pond SL. Evolution of Viral Genomes: Interplay Between Selection, Recombination, and Other Forces. In: Anisimova M, editor. Evolutionary Genomics: Statistical and Computational Methods. New York, NY: Springer; 2019. pp. 427–468. https://doi.org/10.1007/978-1-4939-9074-0_14

82. Minh BQ, Schmidt HA, Chernomor O, Schrempf D, Woodhams MD, von Haeseler A, et al. IQ-TREE 2: New Models and Efficient Methods for Phylogenetic Inference in the Genomic Era. Mol Biol Evol. 2020; 37: 1530–1534. https://doi.org/10.1093/molbev/msaa015 PMID: 32011700

83. Muse SV, Gaut BS. A likelihood approach for comparing synonymous and nonsynonymous nucleotide substitution rates, with application to the chloroplast genome. Mol Biol Evol. 1994; 11: 715–724. https://doi.org/10.1093/oxfordjournals.molbev.a040152 PMID: 7968485

84. Sagulenko P, Puller V, Neher RA. TreeTime: Maximum-likelihood phylodynamic analysis. Virus Evol. 2018; 4. https://doi.org/10.1093/ve/vex042 PMID: 29340210

85. Huerta-Cepas J, Serra F, Bork P. ETE 3: Reconstruction, Analysis, and Visualization of Phylogenomic Data. Mol Biol Evol. 2016; 33: 1635–1638. https://doi.org/10.1093/molbev/msw046 PMID: 26921390

86. Echave J, Wilke CO. Biophysical Models of Protein Evolution: Understanding the Patterns of Evolutionary Sequence Divergence. Annu Rev Biophys. 2017; 46: 85–103. https://doi.org/10.1146/annurev-biophys-070816-033819 PMID: 28301766

87. Crawford KHD, Eguia R, Dingens AS, Loes AN, Malone KD, Wolf CR, et al. Protocol and Reagents for Pseudotyping Lentiviral Particles with SARS-CoV-2 Spike Protein for Neutralization Assays. Viruses. 2020; 12: 513. https://doi.org/10.3390/v12050513 PMID: 32384820

88. Lee JM, Huddleston J, Doud MB, Hooper KA, Wu NC, Bedford T, et al. Deep mutational scanning of hemagglutinin helps predict evolutionary fates of human H3N2 influenza variants. Proc Natl Acad Sci U S A. 2018; 115: E8276–E8285. https://doi.org/10.1073/pnas.1806133115 PMID: 30104379

89. Dingens AS, Crawford KHD, Adler A, Steele SL, Lacombe K, Eguia R, et al. Serological identification of SARS-CoV-2 infections among children visiting a hospital during the initial Seattle outbreak. Nat Commun. 2020; 11: 4378. https://doi.org/10.1038/s41467-020-18178-1 PMID: 32873791